

# The binary fraction in the globular cluster M10 (NGC 6254): comparing core and outer regions <sup>1</sup>

E. Dalessandro<sup>2</sup>, B. Lanzoni<sup>2</sup>, G. Beccari<sup>3</sup>, A. Sollima<sup>4</sup>, F.R. Ferraro<sup>2</sup>, and M. Pasquato<sup>2</sup>

<sup>2</sup> *Dipartimento di Astronomia, Università degli Studi di Bologna, via Ranzani 1, I-40127 Bologna, Italy*

<sup>3</sup> *ESO - European Southern Observatory, Karl-Swarzschild Str. 2, D-85748 Garching bei München, Germany*

<sup>4</sup> *INAF Osservatorio Astronomico di Padova, Vicolo dell'Osservatorio 5, I-35122 Padova, Italy*

24 August, 2011

## ABSTRACT

We study the binary fraction of the globular cluster M10 (NGC 6254) as a function of radius from the cluster core to the outskirts, by means of a quantitative analysis of the color distribution of stars relative to the fiducial main sequence. By taking advantage of two data-sets, acquired with the Advanced Camera for Survey and the Wide Field Planetary Camera 2 on board the Hubble Space Telescope, we have studied both the core and the external regions of the cluster. The binary fraction is found to decrease from  $\sim 14\%$  within the core, to  $\sim 1.5\%$  in a region between 1 and 2 half-mass radii from the cluster centre. Such a trend and the derived values are in agreement with previous results obtained in clusters of comparable total magnitude. The estimated binary fraction is sufficient to account for the suppression of mass segregation observed in M10, without any need to invoke the presence of an intermediate-mass black hole in its centre.

*Subject headings:* binaries: general; globular clusters: individual (M10, NGC6254)

---

<sup>1</sup>Based on observations collected with the NASA/ESA *HST*, obtained at the Space Telescope Science Institute, which is operated by AURA, Inc., under NASA contract NAS5-26555.

## 1. INTRODUCTION

The binary fraction is an essential component in the formation and evolution of dynamically active systems, like globular clusters (GCs). In such dense environments, where stellar gravitational interactions are very frequent, binaries can exert a significant influence on both the dynamical evolution of the system and the properties of its stellar populations.

Being, on average, more massive than the other stars, binaries tend to sink into the highly crowded cluster centers, because of equipartition. The characteristic timescale of this process (the relaxation time) depends on the cluster structure and can be even longer than a Hubble time in the outskirts. Hence, in the outer regions of GCs we essentially expect to observe primordial binary systems, i.e., binaries created as part of the star formation process and evolving undisturbed. In the cluster core, on the other hand, a variety of dynamical processes (exchange interactions, three-body encounters, tidal captures, etc.) can take place, with competing effects on the binary population: binaries can be destroyed, created or just modified (e.g. Hut et al. 1992), with relative efficiencies that still are a matter of debate in the literature (e.g. Ivanova et al. 2005; Hurley et al. 2007; Sollima 2008; Fregeau et al. 2009). In general, however, the gravitational encounters occurring in the core tend to make the binaries harder (more tightly bound), thus providing a central energy source able to slow down the cluster core collapse (Goodman & Hut 1989). Following the N-body simulations of Gill et al. (2008), this energy source could also suppress the mass segregation process, with a detectable effect on the radial behavior of the mass function of main-sequence (MS) stars. Since the same effect could alternatively be due to a central intermediate-mass black hole (IMBH; see also Pasquato et al. 2009; Beccari et al. 2010, hereafter B10), if we can measure the fraction of binaries, then we can say whether or not we need an IMBH to explain the low level of mass segregation that has been observed. Hence, the empirical estimate of the binary fraction in a sample of GCs representative of different environments is a prime ingredient for dynamical models, which help us understand the internal cluster dynamics.

The knowledge of the binary fraction is also crucial for understanding the properties of puzzling objects like blue stragglers, millisecond pulsars and cataclysmic variables, which are all thought to be the by-products of binary evolution (e.g., McCrea 1964; Romani et al. 1987; Ferraro et al. 2001; Leigh et al. 2011, and references therein). In particular, the analysis of the bimodal radial distribution of blue stragglers observed in a number of GCs (e.g., Ferraro et al. 1997, 2004; Dalessandro et al. 2008) suggests that a non-negligible fraction of these stars is generated by primordial binaries, which still orbit in isolation in the cluster outskirts and produce the observed rising branch of the distribution (Mapelli et al. 2004, 2006; Lanzoni et al. 2007a,b). The interpretation of the double blue straggler sequence recently discovered in the core of M30 also requires a significant fraction of primordial binaries (Ferraro et al.

2009).

Despite its implications, however, the binary fraction in GCs still remains badly constrained, because of the challenging observational requirements. The main techniques commonly used for its estimate are: radial velocity variability surveys (e.g. Pryor et al. 1989; Latham 1996; Albrow et al. 2001), searches for eclipsing binaries (e.g. Mateo 1996; Cote et al. 1996), and the study of the distribution of stars along the cluster MS in color-magnitude diagrams (CMDs; e.g., Romani et al. 1991; Bolte 1992; Rubenstein & Bailyn 1997; Bellazzini et al. 2002; Clark, Sandquist & Bolte 2004; Zhao & Bailyn 2005; Sollima et al. 2007; Milone et al. 2008). The first two methods rely on the detection of individual binary systems in a given range of periods and mass ratios. Hence, the nature of these methods leads to intrinsic observational biases and a low detection efficiency. The latter approach relies on the simple fact that, since the flux of unresolved binaries is equal to the sum of the fluxes of the two components, the binaries composed by MS companions are shifted towards brighter magnitudes with respect to the single-star MS. This technique has the advantage of being more efficient and detecting binary systems regardless of their orbital periods and inclinations.

For the present paper we used this latter technique to estimate the binary fraction in the core and the outskirts of M10 (NGC 6254). This is an “ordinary”, dynamically relaxed GC, with absolute visual magnitude  $M_V = -7.48$  (Harris 1996, 2010 edition), central mass density  $\log \rho_0 = 3.8$  ( $\rho_0$  being in units of  $M_\odot/\text{pc}^3$ ; Pryor & Meylan 1993), and half-mass relaxation time  $t_h \sim 0.8$  Gyr (Harris 1996; see also McLaughlin & van der Marel 2005). The deep and high-quality photometry that B10 obtained for both the centre and beyond the half-mass radius, allowed them to study the cluster mass function at different radial distances. The resulting mass-segregation profile is moderately flattened and can be explained by the presence of either an IMBH of  $\sim 10^3 M_\odot$ , or a population of binaries with an initial fraction of 3-5% (B10). Hence, within the framework proposed by Gill et al. (2008), any empirical constraint on the binary content in this system would allow us to assess the possible presence of a central IMBH. In addition, it will provide precious clues and constraints that would be useful for a robust interpretation of the properties the blue-straggler-population in this cluster (Emanuele Dalessandro et al. 2011 in preparation).

The paper is organized as follows. The used data-sets are presented in Section 2. The method adopted to estimate the binary fraction is outlined in Section 3. The results and the discussion are presented in Section 4 and 5.

## 2. THE DATA

The data-set used in the present work (the same as in B10) consists of a sample of  $4 \times 90sec$  images acquired in the F606W ( $V$ ) and  $4 \times 90sec$  images in F814W filters obtained with the Advanced Camera for Surveys (ACS; GO-10775, PI: Sarajedini), complemented with  $2 \times 1100sec$  and  $2 \times 1200sec$  images in F606W and  $2 \times 1100sec$  and  $2 \times 1200sec$  images obtained with the Field Planetary Camera 2 (WFPC2; GO-6113, PI: Paresce) on board the Hubble Space Telescope. The ACS data-set samples the cluster central regions, while the WFPC2 one covers an area located between one and two half-mass radii (see Figure 1). The detailed description of the data reduction, photometric calibration<sup>2</sup> and astrometric solution procedures is given in B10 and the sample used in the present analysis contains the same “bona-fide” stars selected on the basis of the quality of the point-spread-function fitting (as measured by the DAOPHOTII sharpness parameter; Stetson 1987). The CMDs of the two data-sets are shown in Figure 2. Stars brighter than  $I = 16$  and  $I = 19.5$  are saturated in the ACS and WFPC2 samples, respectively. B10 also performed a detailed photometric completeness study, based on artificial star experiments, where artificial stars were added to the original FLT frames and the whole data reduction procedure was repeated. From the resulting catalogue, listing the input and output positions and magnitudes for more than 500,000 artificial stars, B10 estimated that the photometric completeness drops below 50% at  $I \sim 22.5$  in the innermost region of the cluster, and at  $I \sim 25$  for the WFPC2 data-set.

## 3. THE ANALYSIS

In order to estimate the binary fraction of M10, we followed the method extensively described in Bellazzini et al. (2002) and Sollima et al. (2007, hereafter S07). The basic idea is that the magnitude of a binary system corresponds to the luminosity of the primary (more massive) star, increased by the contribution of the companion of an amount that depends on the mass ratio of the two components ( $q = M_2/M_1$ ). In fact, since the stars along the MS follow a mass-luminosity relation, the luminosity of a binary can be written in terms of the mass ratio of the two components. By definition,  $0 < q \leq 1$  and for  $q = 1$  (equal-mass binary) the system appears  $\sim 0.75$  magnitudes brighter than the single component, while the luminosity enhancement decreases for decreasing  $q$ . The spanning of all the possible values of  $q$ , at different magnitudes of the primary component, produces a broadening of the

---

<sup>2</sup>The instrumental  $V$  and  $I$  magnitudes have been calibrated to the VEGAMAG system by following the prescription of Sirianni et al. (2005) and Holtzman et al. (1995) for the ACS and the WFPC2 samples, respectively.

single-star MS, to its bright- and red-hand side. In principle, the ratio between the number of stars lying on the red side of the single-star MS and the total number of stars observed along the “broadened MS” provides the cluster binary fraction. In practice, depending on the photometric error of the data, a minimum value of the mass ratio ( $q_{min}$ ) exists below which it is impossible to observationally distinguish a binary system from a single MS star. Moreover, it is necessary to take into account a number of effects, like stellar blends and the contamination by foreground/background field stars, which can add spurious sources in the CMD.

Indeed, chance superpositions of two stars (blends) can produce a luminosity enhancement that mimics the magnitude shift characteristic of a genuine binary system. In order to correct for this effect we analyzed the distribution of the residuals between the input and the output magnitudes of the artificial star catalogue built by B10 for the completeness study (see previous section). From the asymmetry of the distribution (which is skewed toward brighter output magnitudes because of the blending between artificial and real stars) we estimated that the percentage of blended sources that would mimick binary systems with  $q > q_{min}$ , varies from  $\sim 6\%$  in the core, to less than  $0.2\%$  in the external regions.

B10 also estimated the Galactic field contamination in the direction of M10, finding that it is very low: even in the worst case (the WFPC2 data-set), where the number of cluster sources is small, the field stars are just  $\sim 3\%$  of the total sample. Despite such a low value, for a proper measurement of the binary fraction we performed a detailed study of the field contamination as a function of the magnitude. From the Galaxy model of Robin et al. (2003)<sup>3</sup> we retrieved a catalogue covering an area of  $0.5 \text{ deg}^2$  in the direction of M10, and we randomly extracted two sub-samples of synthetic stars, scaled to the fields of view of the ACS and WFPC2 data-sets. Their magnitudes were converted from the Johnson to the VEGAMAG photometric system adopting the prescriptions of Sirianni et al. (2005). Finally, by exploiting the artificial-star catalogue used for the completeness study<sup>4</sup> (Sect. 2), we obtained a catalogue of synthetic field stars that includes the observational biases (incompleteness and blending), for both the ACS and WFPC2 data-sets.

Once all the contaminant effects are taken into account, the binary fraction was estimated as the number of stars in the “*binary population*” divided by the total number of stars, i.e., binaries plus genuine, single, MS stars (hereafter the “*MS population*”). The “MS

---

<sup>3</sup>publicly available at <http://model.obs-besancon.fr/>

<sup>4</sup>For each considered synthetic field star, we randomly extracted an artificial object with similar magnitude ( $\Delta I < 0.1$ ) and we assigned the shifts between its input and output magnitudes to the field star, in a effort to mimick and take into account the effects of completeness and blending.

population” is defined as the set of stars having a color difference from the MS ridge line (MSRL) smaller than three times the typical photometric error at that magnitude level (see Figure 3). The operational definition of the “binary population” is given in Sects. 4.1 and 4.2.

## 4. RESULTS

The high photometric quality and the spatial coverage of the data-sets previously described allowed us to study the binary fraction at different distances from the cluster centre. In particular, here we have defined three concentric annuli bounded by the core radius and the half-mass radius. The adopted centre of gravity and structural parameters have been recently determined from resolved star counts (Dalessandro et al. 2011): the coordinates of the centre are  $\alpha_{J2000} = 16^{\text{h}} 57^{\text{m}} 8.92^{\text{s}}$ ,  $\delta_{J2000} = -4^{\circ} 5' 58.07''$ ; the core, half-mass and tidal radii are  $r_c = 48''$ ,  $r_h = 147''$ , and  $r_t = 19.3'$ , respectively. This center is located at  $\sim 3.5''$  North-West from the one quoted by Goldsbury et al 2010, a difference that has no impact on the following analysis and the obtained results. Hence, the first two radial bins ( $r < r_c$  and  $r_c < r < r_h$ ) are sampled by the ACS data-set, while the third one ( $r > r_h$ ) is covered by the WFPC2 data (see Fig. 1). Since the two data-sets have different saturation and completeness levels (see Sect. 2), we performed the analysis in two different magnitude ranges: the adopted cuts along the MSRL are  $18.8 < I < 21.5$  for the ACS sample, and  $20.3 < I < 23$  for the WFPC2 one (see Figs. 2 and 3). These intervals define what we call the “*full* magnitude range” of the two data-sets. Then, with the aim of having an interval of magnitudes in common between the two samples where to directly compare the computed binary fractions, we considered three magnitude sub-ranges defined as follows: a “*bright* range” corresponding to  $18.8 < I < 20.3$ , an “*intermediate* range” at  $20.3 < I < 21.5$ , and a “*faint* range” at  $21.5 < I < 23$  (all the quoted magnitude values are measured along the MSRL). As is apparent from Figs. 2 and 3, the *bright* range is probed only by the ACS data-set, the *faint* range is found only in the WFPC2 sample, while the *intermediate* range is in common between the two.

### 4.1. The minimum binary fraction

We first estimated the *minimum binary fraction* ( $\xi_{min}$ ), which is the fraction of binary systems with a mass ratio  $q_{min}$  large enough to make them clearly distinguishable from the single-star MS. It is clear that the value of  $q_{min}$  depends directly on the photometric errors and  $\xi_{min}$  represents only a sub-sample of the whole population of binaries, but it has

the advantage of being a purely observational quantity. In this case we define the “*binary population*” as the set of stars located in the CMD between the following boundaries (see gray region in Fig. 3): the left-hand boundary is the line corresponding to a color difference from the MSRL equal to three times the photometric error at any magnitude level (right dashed line); the right-hand boundary is the line at a color difference from the equal-mass binary sequence equal to three times the photometric error; the upper and lower boundaries are set by the largest and the smallest primary mass (corresponding to the quoted bright and faint cuts of the various magnitude ranges along the MSRL), combined with all the possible mass ratios. In other words, the “binary population” includes all binary systems with primary mass set by the considered magnitude ranges and with  $q_{min} \leq q \leq 1$ , also taking into account the effect of photometric errors.

For each of the considered radial bins and magnitude ranges we estimated the minimum binary fraction by performing all the steps described in Sect. 3 and, in much more detail, in S07. The results are presented in Table 1. As is apparent,  $\xi_{min}$  monotonically decreases from the center to the outskirts, in agreement with previous findings and with theoretical predictions (see Sect. 5). In the *full* magnitude range, such a radial variation ranges from  $\sim 6\%$  at  $r < r_c$ , to  $\sim 1\%$  at  $r > r_h$ . There also seems to be a trend with magnitude, especially in the central bin, where  $\xi_{min}$  varies from  $\sim 8\%$  in the *bright* range, to  $\sim 5\%$  in the *intermediate* one.

However, since the photometric error depends on magnitude, the value of  $q_{min}$  changes in the considered luminosity ranges: for decreasing luminosity,  $q_{min}$  varies from 0.5 to 0.6 in both the ACS and the WFPC2 samples. Hence, the derived values of  $\xi_{min}$  are neither strictly comparable to one other, nor to the estimates presented in different works. We have therefore computed the fraction of binaries with mass ratios larger than a fixed value  $q = 0.6$  ( $\xi_{\geq 0.6}$ ). This value has been chosen as a compromise between having enough statistics and avoiding contamination from single stars (indeed, the line corresponding to  $q = 0.6$  in the CMD always runs to the right-hand side of the MS population boundary). In this case the “binary population” is made up of stars that, in the CMD, are located between the line of constant  $q = 0.6$  (left boundary; see dotted lines in Fig. 3) and the right-hand boundary defined above. Its ratio with respect to the total number of stars gives the fraction of binaries with  $q \geq 0.6$ , which is presented in Table 2. Obviously, the obtained values are smaller than the corresponding minimum fractions  $\xi_{min}$  in Table 1. We also note that the same behaviors discussed above are still present, thus again suggesting that the trend with magnitude could be real. One possible explanation for the trend with magnitude could be that *bright* range systematically samples more massive stars, which are also expected to be more centrally segregated.

## 4.2. The global binary fraction

In order to estimate the overall binary content of M10, independently of the value of  $q$ , we also computed the *global binary fraction* ( $\xi_{TOT}$ ). This requires us to perform simulations of single and binary star populations assuming different input values of the global binary fraction ( $\xi_{in}$ ) and then determining  $\xi_{TOT}$  from the comparison between the artificial and the observed CMDs: the value of  $\xi_{in}$  that provides the best match between the two CMDs is adopted as the global binary fraction  $\xi_{TOT}$  (see Bellazzini et al. 2002 and S07 for a detailed description of the procedure).

Once we assumed an input value of the binary fraction ( $\xi_{in}$ ), for each of the considered radial and magnitude bins we have built a sample of  $N_{MS}$  and  $N_{bin}$  stars, with  $N_{bin} = N\xi_{in}$ ,  $N$  being the number of observed objects (after having taken into account the number of contaminating field stars, discussed in Sect. 3) in that bin, and  $N_{MS}$  being  $N(1 - \xi_{in})$ . The MS stars have been simulated by randomly extracting  $N_{MS}$  values of the mass from the present-day cluster mass function derived by B10<sup>5</sup>, and transforming the masses into luminosities by using the Baraffe et al. (1997) isochrones. Then, from the artificial-star catalogue previously described, we have randomly selected an object with similar ( $\Delta I < 0.1$ ) magnitude and, if recovered, we assigned its output  $I$  and  $V$  magnitudes to the considered MS star. In order to simulate the binary systems we randomly extracted  $N_{bin}$  values of the mass of the primary component from the Kroupa (2002) initial mass function, and  $N_{bin}$  values of the binary mass ratio from the  $f(q)$  distribution observed by Fisher et al. (2005) in the solar neighborhood, thus also obtaining the mass of the secondary. After transforming masses into luminosities and summing up the fluxes of the two components, an object with similar magnitude was randomly extracted from the artificial-star catalogue and, if recovered by the photometric analysis, the shifts between its input and output magnitudes were assigned to the considered binary system. Finally, the field stars were added to the sample. The result of this procedure is a list of synthetic stars with the same characteristics of real stars and containing a given fraction of binaries ( $\xi_{in}$ ). To be precise, the MSs of the resulting artificial CMDs are narrower than the observed ones, because the formal photometric errors of the artificial star catalogue systematically underestimate the true observational uncertainties. This is apparent in Figure 4, where, for the magnitude range  $19 < I < 19.5$ , the histogram

---

<sup>5</sup>B10 suggested that for stars below  $0.5M_{\odot}$ , the slope of the mass function decreases from 0.23 to  $-0.83$  moving from the inner to the outer regions (for reference, the slope of the canonical Salpeter mass function would be  $-2.35$ ). In order to understand how the assumed mass function may affect the binary fraction estimates, we have re-computed  $\xi_{TOT}$  by adopting the core mass function for the whole cluster. Within the errors, the resulting values of  $\xi_{TOT}$  turn out to be in agreement with those presented in Table 3, thus guaranteeing that the global binary fraction is just mildly sensitive to changes in the mass function.



corresponds to the distribution of the observed color differences  $\Delta(V - I)$  with respect to the MSRL, the solid line is the best-fitting Gaussian of the blue-side of this distribution (gray histogram; the red-side has been ignored because it also includes the contribution of binaries and blends), and the dashed line is a Gaussian with a dispersion obtained by adopting the formal photometric error of the artificial star catalogue. In order to correct for this bias and adopt realistic values of the photometric uncertainty, we increased the formal errors  $\sigma_I$  and  $\sigma_V$  thus to reproduce the observed error distribution as a function of magnitude. As a check, we verified that the width of the resulting color distribution with respect to the MSRL well matches the observed one. An example of the synthetic CMD thus obtained, compared to the observed one is shown in Fig. 5. From the simulated catalogue we then computed the ratio  $r_{sim} = N_{bin}^{sim}/N_{MS}^{sim}$  between the number of synthetic stars belonging to the “binary population” defined in Sect. 4.1, and that of the synthetic “MS population”. The same was done for the observed data-sets, thus obtaining  $r_{obs} = N_{bin}^{obs}/N_{MS}^{obs}$ .

For every value of  $\xi_{in}$ , from 0.5% to 25% with steps of 0.5%, the entire procedure was repeated 100 times. Then, the penalty function  $\chi^2(\xi_{in})$  was computed as the summation of  $(r_{sim,i} - r_{obs})^2$  for  $i = 1, 100$ , and the associated probability  $P(\xi_{in})$  was derived. To illustrate this, Figure 6 shows the distribution of  $P$  as a function of the adopted values of  $\xi_{in}$ , ranging from 3% to 10%. The mean of the best-fitting Gaussian gives the global binary fraction ( $\xi_{TOT}$ ) and its dispersion has been adopted as the error. The values of  $\xi_{TOT}$  obtained in the various radial and magnitude ranges are reported in Table 3. The global binary fraction shows the same radial behavior observed for  $\xi_{min}$ , varying from  $\sim 14\%$  or  $\sim 10\%$  in the cluster core (for the *full* and the *intermediate* magnitude ranges, respectively), down to  $\sim 1.5\%$  in the outskirts (for both). As before we find a dependence of the binary fraction on the magnitude. This could be an effect of mass segregation, since the average binary mass in the *bright*, *intermediate* and *faint* ranges is  $M \sim 1.1, 0.8, 0.5M_{\odot}$ , respectively. However it could also depend on the assumed mass-ratio distribution and the estimate of blended sources, and future studies will be required to resolve this.

## 5. DISCUSSION

We have presented a homogeneous analysis of the binary fraction in M10 as a function of the radial distance from the cluster centre, from the core region, out to  $\sim 2r_h$ . Within the errors, the derived *core* binary fraction is consistent with that measured in other GCs, which have typical values of  $\xi_{TOT}$  spanning from  $\sim 10\%$  to  $\sim 25\%$  (S07; Davis et al. 2008) but it is significantly smaller than that estimated for the faintest clusters in the sample of Sollima et al. (2007), which reach also binary fractions  $\xi_{TOT} \sim 50\%$ . This is in agreement

with the quoted anti-correlation between binary fraction and total luminosity (Milone et al. 2008; Sollima 2008; Sollima et al. 2010). Also the binary fraction beyond the half-mass radius ( $\sim 1\%$ ) is consistent with previous estimates in GCs (see Table 1 Davis et al. 2008).

The *minimum* binary fraction decreases from  $\sim 6\%$  within  $r_c$ , to  $\sim 1\%$  beyond the half-mass radius. An analogous trend was found for the fraction of binaries with  $q \geq 0.6$  and for the *global* binary fraction (Fig. 7), the latter varying from  $\sim 14\%$  to  $\sim 1.5\%$  from the core to beyond the half-mass radius. Such a radial behavior is in agreement with what has been previously found in the few other GCs where this kind of investigation has been performed (Rubenstein & Bailyn 1997; Bellazzini et al. 2002; Zhao & Bailyn 2005; Sommariva et al. 2009, and references in Table 1 of Davis et al. 2008). It is also in agreement with the expectations of dynamical models, where the effect is essentially due to the mass-segregation process, which leads to an increase in the number of binaries in the cluster cores (e.g., Hurley et al. 2007; Sollima 2008; Fregeau et al. 2009; Ivanova 2011). Indeed, the half-mass relaxation time of M10 ( $\sim 0.8$  Gyr, Harris 1996; see also Gnedin et al. 1999; McLaughlin & van der Marel 2005) is just a small fraction ( $\sim 4\%$ ) of the cluster age ( $t \sim 13$  Gyr; Dotter et al. 2010), so it seems safe to conclude that the system has already had time to achieve equipartition.

By comparing the radial variation of the MS stellar mass function derived from the observations, with that obtained in N-body simulations, B10 suggested that either an IMBH or a population of binaries should be present and act as a central energy source in M10, suppressing the mass-segregation profile. In particular, the shallow mass-segregation profile could be modeled without an IMBH only when the simulations started with a primordial binary fraction of about  $3 - 5\%$ . Within this framework, in Figure 7 we compare our derived values of  $\xi_{TOT}$ , with those obtained from the dynamical evolution of the  $5\%$  primordial binary population in the 32K particle simulation of B10. For a proper comparison we considered a simulation snapshot at  $\sim 7$  relaxation times, and only those binaries made of two MS stars and with the primary component in the mass range  $0.44 \div 0.56 M_\odot$ , corresponding to the lower and upper cuts of the *intermediate* magnitude range along the MSRL. The resulting binary fractions for the three considered radial bins are:  $\xi_{N-body} = (0.070 \pm 0.02)$ ,  $(0.032 \pm 0.007)$ ,  $(0.026 \pm 0.006)$ , from the centre to the outskirts. It is apparent from Fig. 7 that the observed binary fraction is larger than the simulated one, especially in the core. This indicates that the binary content of M10 is indeed sufficient to account for the observed mass segregation suppression, with no need to invoke an IMBH as additional energy source.

We thank the anonymous referee for the careful reading and the useful comments that improved the presentation of this work. This research is part of the project *COSMIC-LAB* funded by the *European Research Council* (under contract ERC-2010-AdG-267675). The financial contribution of *Istituto Nazionale di Astrofisica* (INAF, under contract PRIN-

INAF 2008) and the *Agenzia Spaziale Italiana* (under contract ASI/INAF I/009/10/0) is also acknowledged.

## REFERENCES

- Albrow M. D., Gilliland R. L., Brown T. M., Edmonds P. D., Guhathakurta P., Sarajedini A., 2001, *ApJ*, 559, 1060
- Baraffe, I., Chabrier, G., Allard, F., & Hauschildt, P. H. 1997, *A&A*, 327, 1054
- Beccari, G., Pasquato, M., De Marchi, G., Dalessandro, E., Trenti, M., & Gill, M. 2010, *ApJ*, 713, 194 (B10)
- Bellazzini, M., Fusi Pecci, F., Messineo, M., Monaco, L., & Rood, R. T. 2002, *AJ*, 123, 1509
- Bolte C. D., 1992, *ApJS*, 82, 145
- Clark L. L., Sandquist E. L., Bolte M., 2004, *AJ*, 138, 3019
- Cote P., Pryor C., McClure R. D., Fletcher J. M., Hesser J. E., 1996, *AJ*, 112, 574
- Dalessandro E., Lanzoni, B., Ferraro, F.R., Rood, R.T., Milone, A., Piotto, G., & Valenti E. et al. 2008, *ApJ*, 6677, 1069
- Davis, D. S., Richer, H. B., Anderson, J., Brewer, J., Hurley, J., Kalirai, J. S., Rich, R. M., & Stetson, P. B. 2008, *AJ*, 135, 2155
- Dotter, A., et al. 2010, *ApJ*, 708, 698
- Ferraro, F. R., et al. 1997, *A&A*, 324, 915
- Ferraro, F. R., Possenti, A., D’Amico, N., & Sabbi, E. 2001, *ApJ*, 561, L93
- Ferraro, F. R., Beccari, G., Rood, R. T., Bellazzini, M., Sills, A., & Sabbi, E. 2004, *ApJ*, 603, 127
- Ferraro, F. R., et al. 2009, *Nature*, 462, 1028
- Fisher J., Schroder K.P., Smith R.C., 2005, *MNRAS*, 361, 495
- Fregeau, J. M., Ivanova, N., & Rasio, F. A. 2009, *ApJ*, 707, 1533
- Gill, M., Trenti, M., Miller, M. C., van der Marel, R., Hamilton, D., & Stiavelli, M. 2008, *ApJ*, 686, 303

- Gnedin, O. Y., Lee, H. M., & Ostriker, J. P. 1999, *ApJ*, 522, 935
- Goldsbury, R., Richer, H. B., Anderson, J., Dotter, A., Sarajedini, A., & Woodley, K. 2010, *AJ*, 140, 1830
- Goodman, J., & Hut, P. 1989, *Nature*, 339, 40
- Holtzman, J. A., Burrows, C. J., Casertano, S., Hester, J. J., Trauger, J. T., Watson, A. M., & Worthey, G. 1995, *PASP*, 107, 1065
- Harris, W.E. 1996, *AJ*, 112, 1487 (2010 edition)
- Hurley, J. R., Aarseth, S. J., & Shara, M. M. 2007, *ApJ*, 665, 707
- Hut, P., et al. 1992, *PASP*, 104, 981
- Ivanova, N., Belczynski, K., Fregeau, J. M., & Rasio, F. A. 2005, *MNRAS*, 358, 572
- Ivanova, N. 2011, in “Binary Star Evolution: Mass Loss, Accretion and Mergers”, V. Kalogera and M. van der Sluys Eds; *AIP Conf. Ser.*
- Kroupa P., 2002, *Sci*, 295, 82
- Lanzoni, B., Dalessandro, E., Ferraro, F. R., Mancini, C., Beccari, G., Rood, R. T., Mapelli, M., & Sigurdsson, S. 2007a, *ApJ*, 663, 267
- Lanzoni, B., et al. 2007b, *ApJ*, 663, 1040
- Latham, D. W., 1996, in *The Origins, Evolution, and Destinies of Binary Stars in Clusters*, E.F. Milone and J.C. Mermilliod eds., *ASP, S. Francisco, ASP Conf. Ser.*, vol. 90, p. 31
- Leigh, N., Sills, A., & Knigge, C. 2011, *arXiv:1105.5388*
- Mapelli, M., Sigurdsson, S., Colpi, M., Ferraro, F. R., Possenti, A., Rood, R. T., Sills, A., & Beccari, G. 2004, *ApJ*, 605, L29
- Mapelli, M., Sigurdsson, S., Ferraro, F. R., Colpi, M., Possenti, A., & Lanzoni, B. 2006, *MNRAS*, 373, 361
- Mateo M., 1996 in “The Origins, Evolution and Destinies of Binary Stars in Clusters”, E. F. Milone & J. C. Mermilliod eds., *San Francisco ASP Conf. Ser.*, 90, 21
- McCrea, W. H. 1964, *MNRAS*, 128, 147

- McLaughlin, D. E., & van der Marel, R. P. 2005, *ApJS*, 161, 304
- Milone, A. P., Piotto, G., Bedin, L. R., & Sarajedini, A. 2008, *Mem. Soc. Astron. Italiana*, 79, 623
- Pasquato, M., et al. 2009, *ApJ*, 699, 1511
- Pryor, C., McClure, R. D., Hesser, J. E., & Fletcher, J. M. 1989, *Dynamics of Dense Stellar Systems*, 175
- Pryor, C., & Meylan, G. 1993, *Structure and Dynamics of Globular Clusters*, 50, 357
- Robin A. C., Reil  C., Derri re S., Picaud S., 2003, *A&A*, 409, 523
- Romani, R. W., Kulkarni, S. R., & Blandford, R. D. 1987, *Nature*, 329, 309
- Romani R. W., Weinberg M. D., 1991, *ApJ*, 372, 487
- Rubenstein, E. P., & Bailyn, C. D. 1997, *ApJ*, 474, 701
- Sirianni et al., 2005, *PASP*, 117, 1049
- Sollima, A., Beccari, G., Ferraro, F. R., Fusi Pecci, F., & Sarajedini, A. 2007, *MNRAS*, 380, 781 (S07)
- Sollima, A. 2008, *MNRAS*, 388, 307
- Sollima, A., Carballo-Bello, J. A., Beccari, G., Ferraro, F. R., Pecci, F. F., & Lanzoni, B. 2010, *MNRAS*, 401, 577
- Sommariva, V., Piotto, G., Rejkuba, M., Bedin, L. R., Heggie, D. C., Mathieu, R. D., & Villanova, S. 2009, *A&A*, 493, 947
- Stetson, P. B. 1987, *PASP*, 99, 191
- Zhao, B., & Bailyn, C. D. 2005, *AJ*, 129, 1934

Radial bin	<i>full</i> <i>mag range</i>	<i>bright</i> (18.8 < <i>I</i> < 20.3)	<i>intermediate</i> (20.3 < <i>I</i> < 21.5)	<i>faint</i> (21.5 < <i>I</i> < 23)
$r < r_c$	$(6.3 \pm 0.4)\%$	$(7.6 \pm 0.5)\%$	$(4.6 \pm 0.5)\%$	–
$r_c < r < r_h$	$(3.6 \pm 0.2)\%$	$(3.9 \pm 0.2)\%$	$(3.1 \pm 0.2)\%$	–
$r > r_h$	$(1.2 \pm 0.3)\%$	–	$(1.5 \pm 0.6)\%$	$(1.1 \pm 0.3)\%$

Table 1: Minimum binary fraction ( $\xi_{min}$ ) of M10 in the three considered radial bins and the magnitude ranges defined in a Sect. 3.

Radial bin	<i>full</i> <i>mag range</i>	<i>bright</i> (18.8 < <i>I</i> < 20.3)	<i>intermediate</i> (20.3 < <i>I</i> < 21.5)	<i>faint</i> (21.5 < <i>I</i> < 23)
$r < r_c$	$(5.2 \pm 0.3)\%$	$(6.2 \pm 0.5)\%$	$(4.2 \pm 0.5)\%$	–
$r_c < r < r_h$	$(3.0 \pm 0.2)\%$	$(3.2 \pm 0.2)\%$	$(2.9 \pm 0.2)\%$	–
$r > r_h$	$(0.8 \pm 0.2)\%$	–	$(0.7 \pm 0.4)\%$	$(1.0 \pm 0.3)\%$

Table 2: As in Table 1, but for the fraction of binaries with mass ratio  $q \geq 0.6$  ( $\xi_{q \geq 0.6}$ ).

Radial bin	<i>full</i> <i>range</i>	<i>bright</i> ( $18.8 < I < 20.3$ )	<i>intermediate</i> ( $20.3 < I < 21.5$ )	<i>faint</i> ( $21.5 < I < 23$ )
$r < r_c$	$(13.8 \pm 1.4)\%$	$(15.1 \pm 1.9)\%$	$(10.0 \pm 1.6)\%$	—
$r_c < r < r_h$	$(7.4 \pm 0.6)\%$	$(7.6 \pm 0.8)\%$	$(6.3 \pm 0.6)\%$	—
$r > r_h$	$(1.5 \pm 0.6)\%$	—	$(1.5 \pm 1.0)\%$	$(1.5 \pm 0.7)\%$

Table 3: Global binary fraction ( $\xi_{TOT}$ ) of M10 for the considered radial and magnitude intervals.

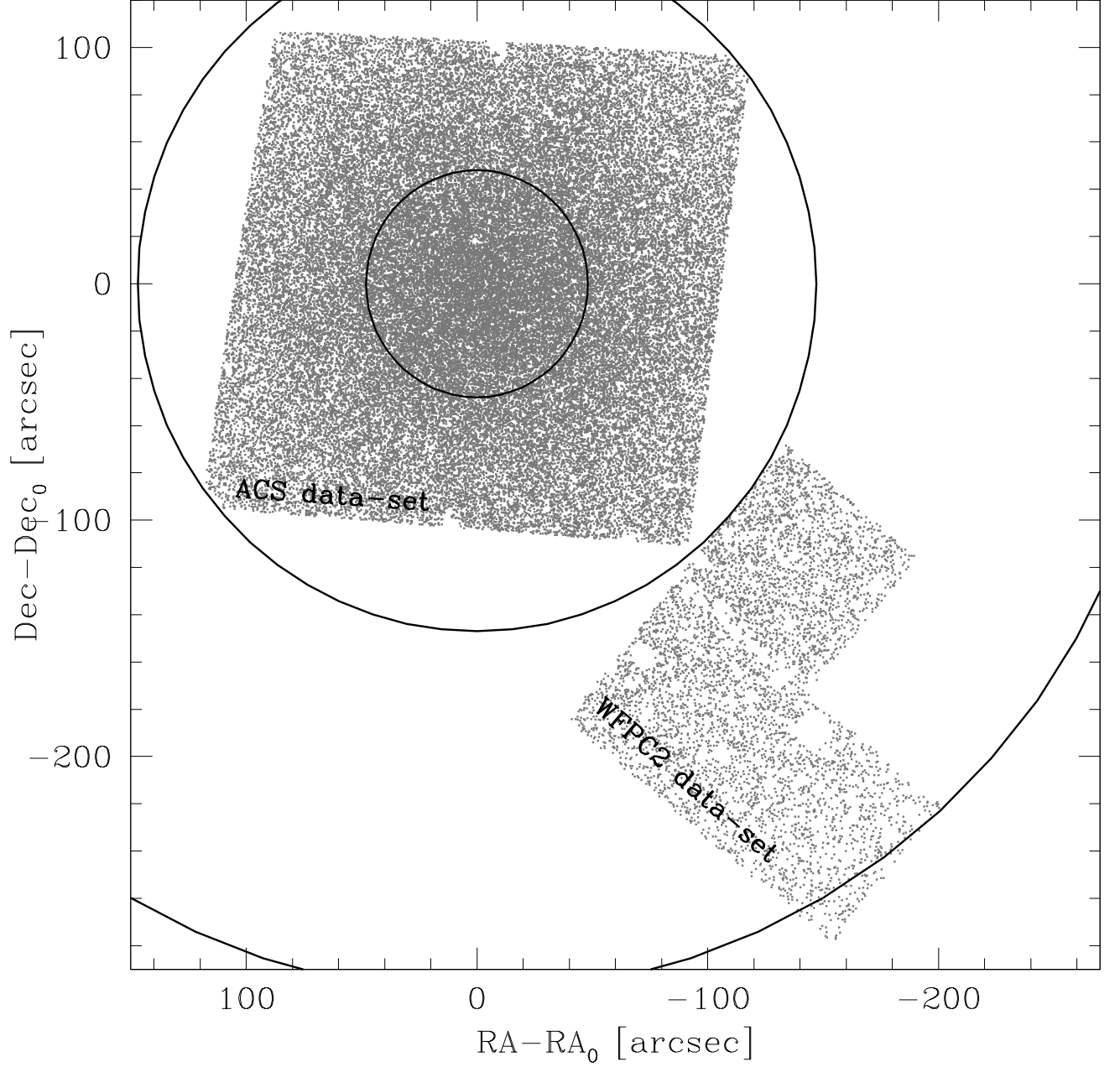


Fig. 1.— Map of the ACS and WFPC2 data-sets. The two circles mark the position of the core and half-mass radii ( $r_c = 48''$ ,  $r_h = 147''$ ). The ACS data-set samples the inner portion of M10 out to  $\sim r_h$ , while the WFPC2 data-set (consisting of the data acquired with the three wide field cameras) covers a region between one and two half-mass radii.



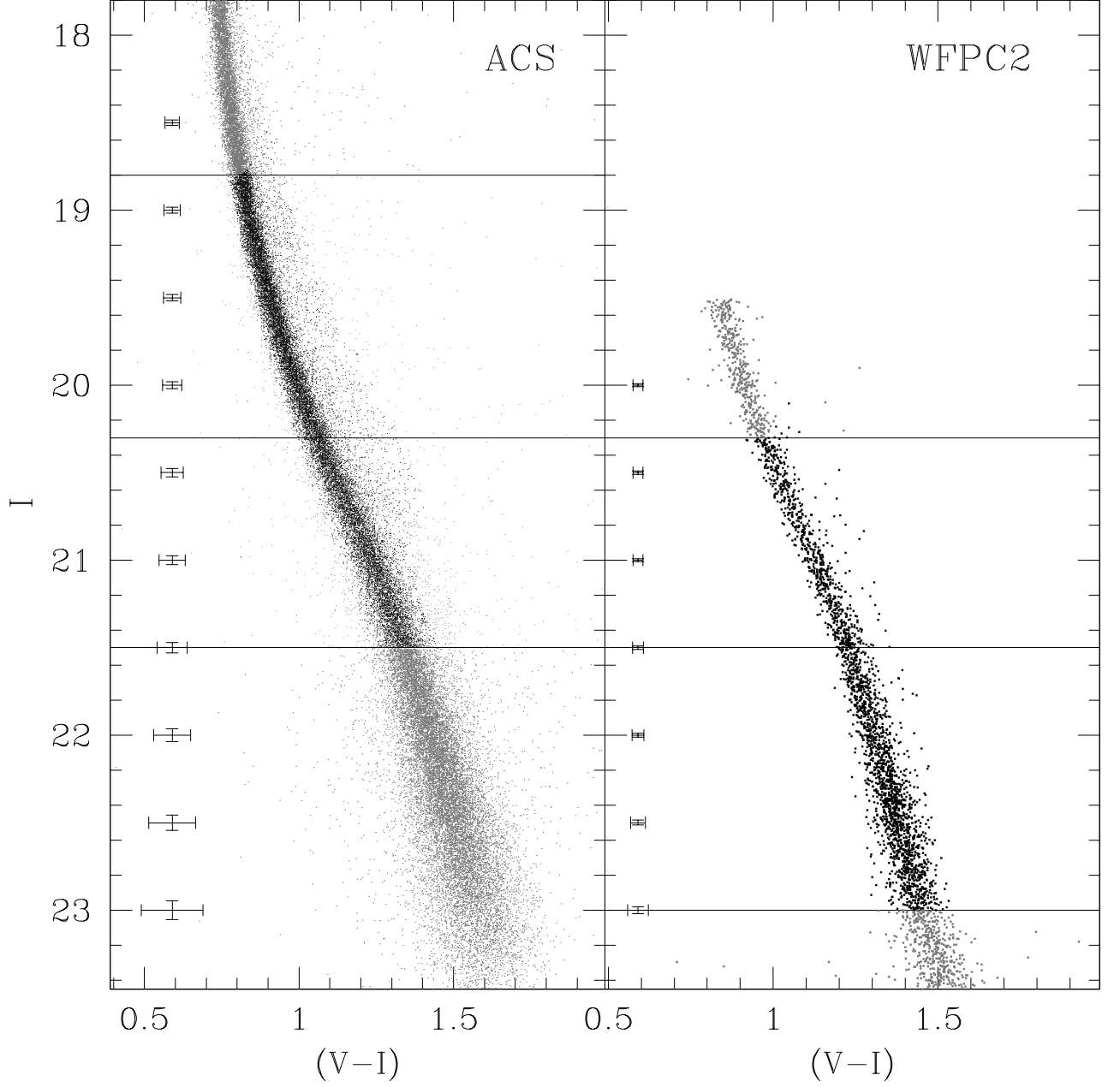


Fig. 2.— CMDs of the ACS and WFPC2 data-sets. The stars used to estimate the binary fraction are plotted in black. The three horizontal lines mark the values along the MSRL that separate the magnitude ranges considered in the work (see Sect. 3). The photometric errors at different magnitude levels are shown.

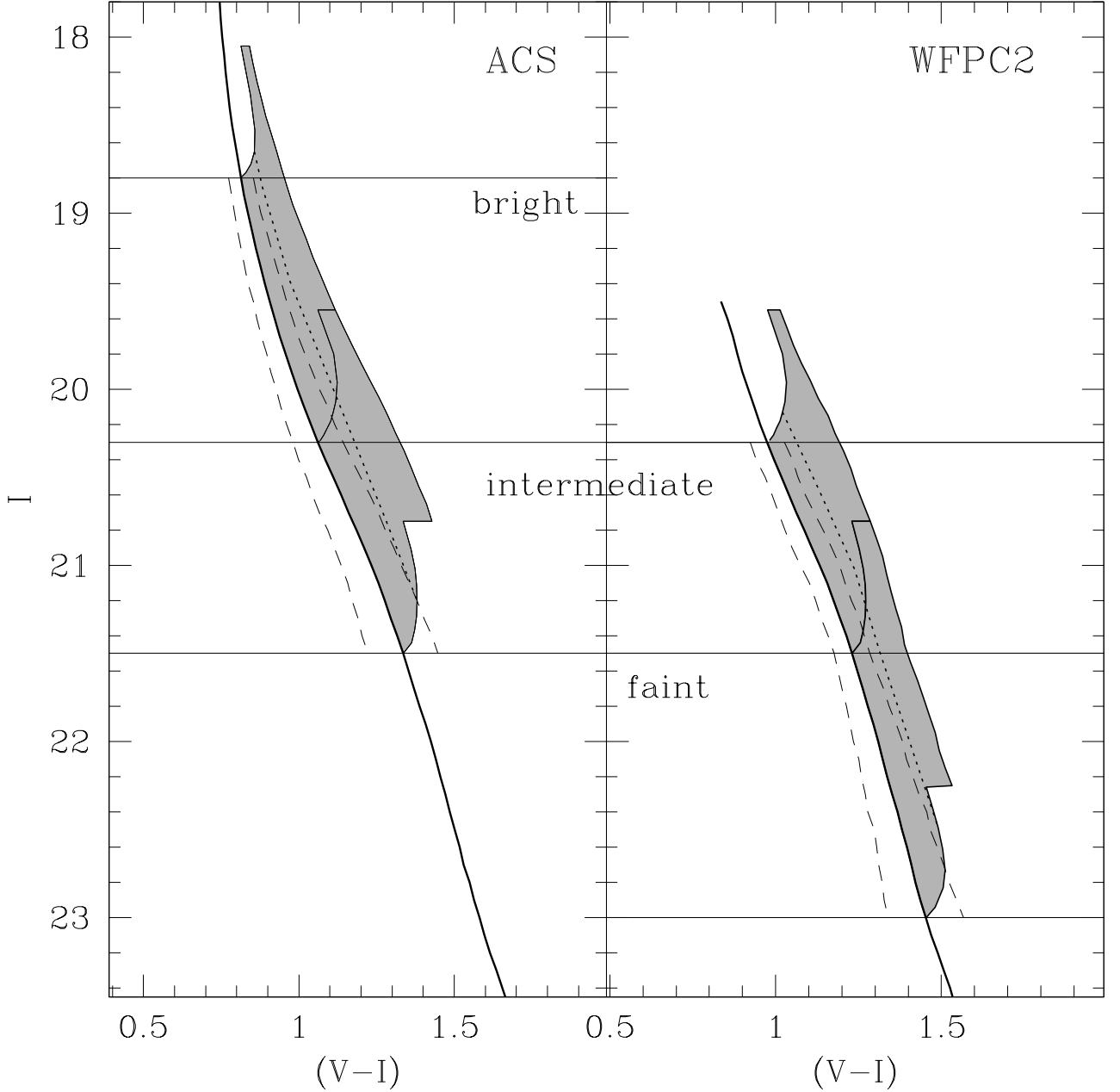


Fig. 3.— Selection boxes used to define the “MS population” and the “binary population” for the two data-sets. The thick solid line marks the MSRL. The dashed lines bound the “MS population”, made of stars with a color difference from the MSRL smaller than three times the typical photometric error at that magnitude level (see Sect. 3). The gray region marks the “binary population” selection box, with its left-hand side corresponding to the redder boundary of the MS population region (right-hand dashed line) and its right-hand side corresponding to the equal-mass binary boundary shifted to the red by three times the photometric error (Sect. 4.1). The dotted line represents the locus defined by binary systems with mass-ratio  $q = 0.6$ .

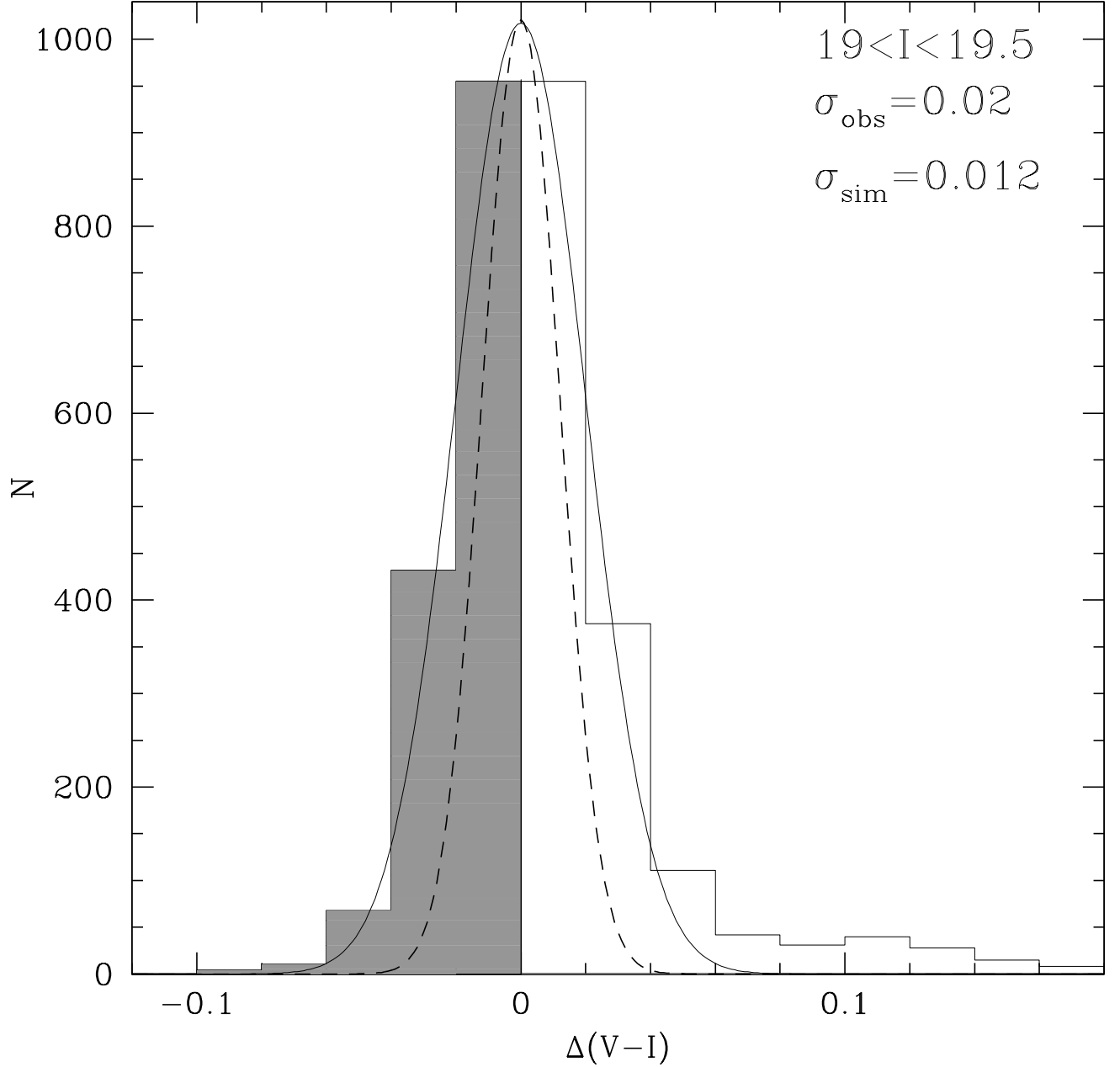


Fig. 4.— Observed color distribution of MS stars with respect to the MSRL, in the magnitude range  $19 < I < 19.5$  for the ACS data-set (histogram). The solid line corresponds to the Gaussian that best-fits the blue-side of the observed distribution (gray histogram), while the red-side has not be taken into account since it also includes the contribution of binaries. The dashed line is a Gaussian with a dispersion equal to the formal photometric error derived from the artificial star simulations (B10).

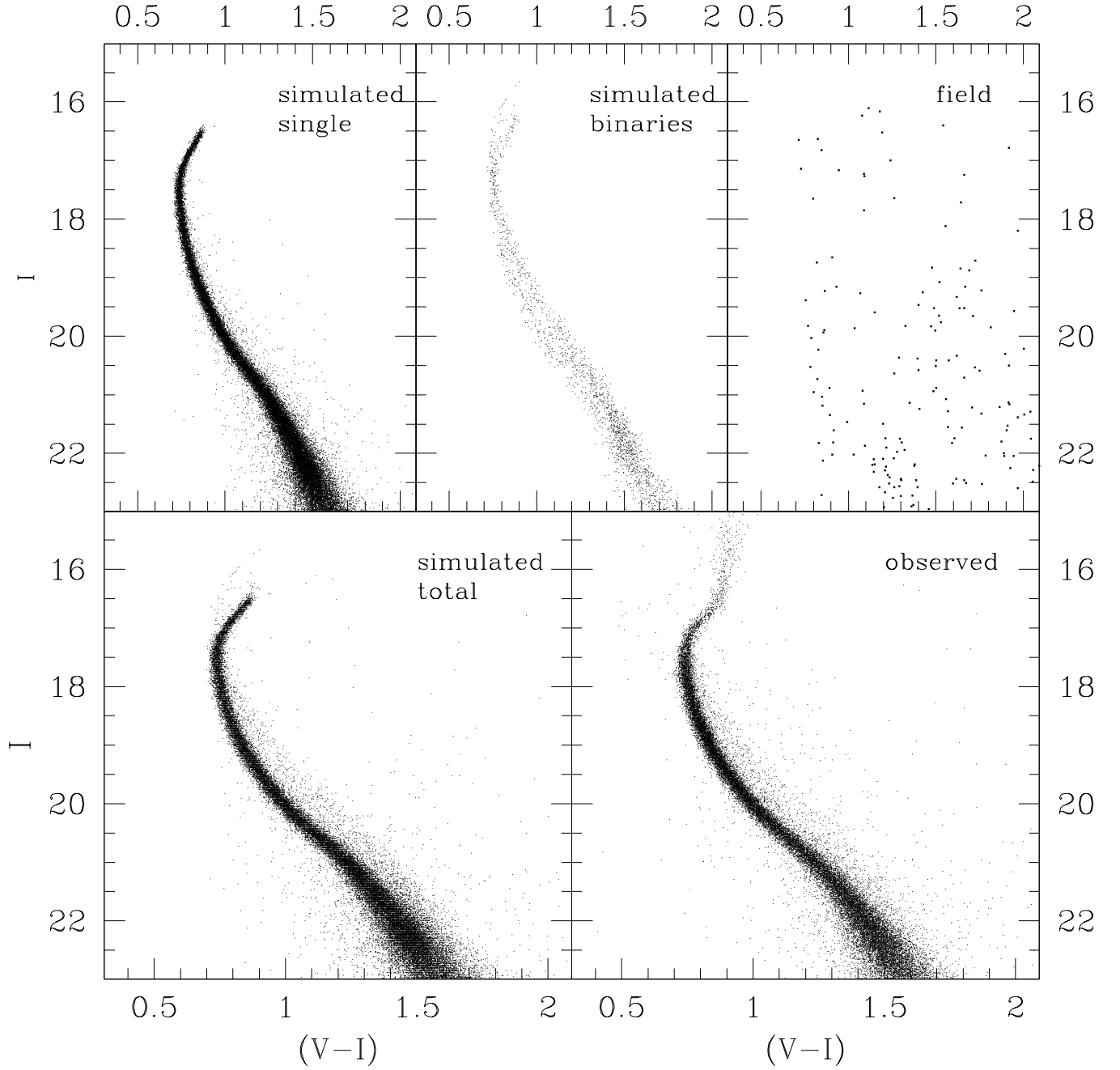


Fig. 5.— CMDs corresponding to the simulated single MS stars, binaries, and field stars for the case of the ACS sample,  $r_c < r < r_h$ , and  $\xi_{\text{in}} = 6.3$  (upper panels). The lower panels show the comparison between the combined synthetic CMD (left-hand side) and the observed one (right-hand side).

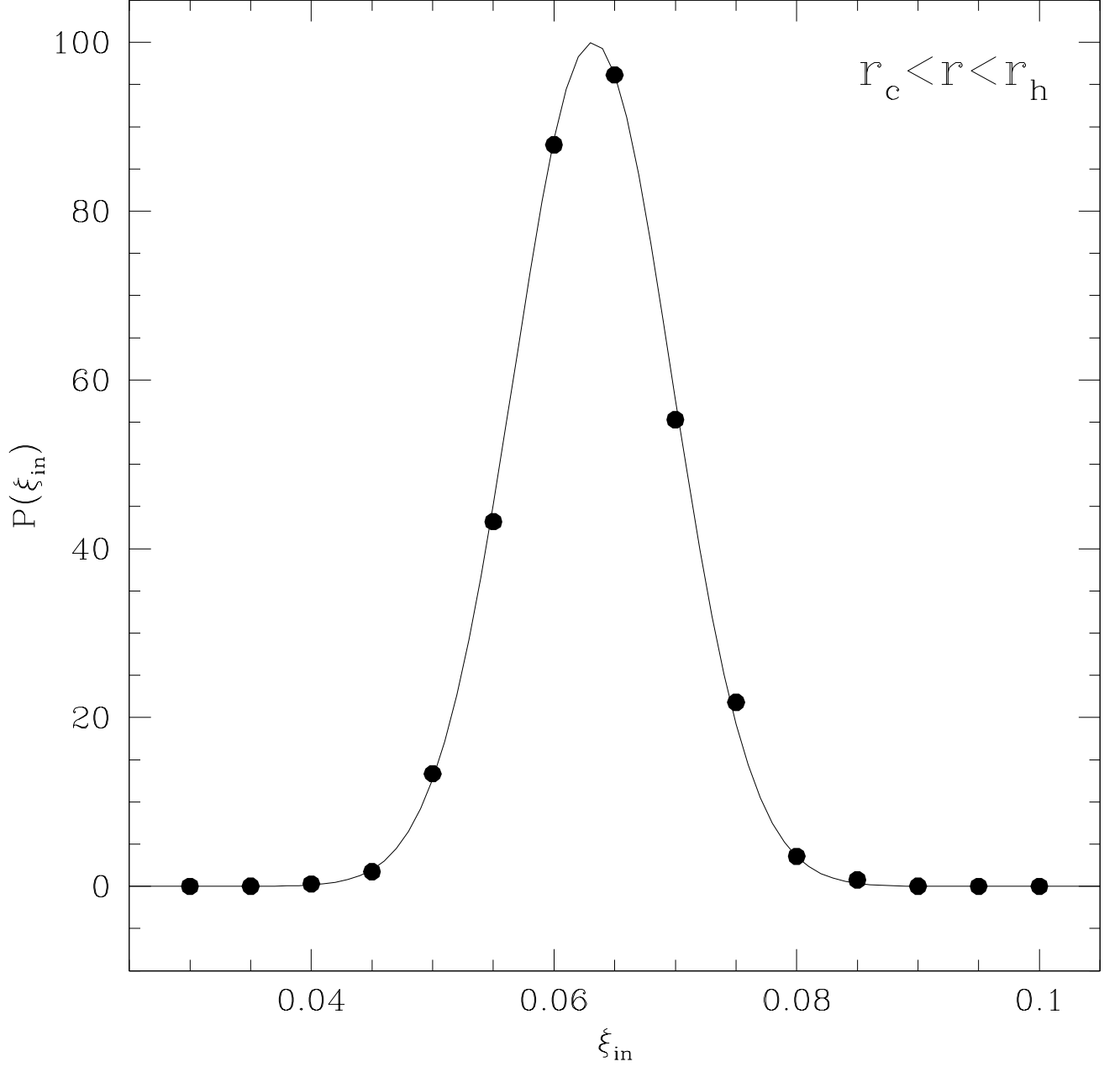


Fig. 6.— Probability distribution of the adopted input binary fractions  $\xi_{\text{in}}$ , for the case of the ACS sample,  $r_c < r < r_h$  and the *intermediate* magnitude range. The mean and the dispersion of the best-fitting Gaussian give the global binary fraction and its error:  $\xi_{\text{TOT}} = (6.3 \pm 0.6)\%$  (see Table 3).

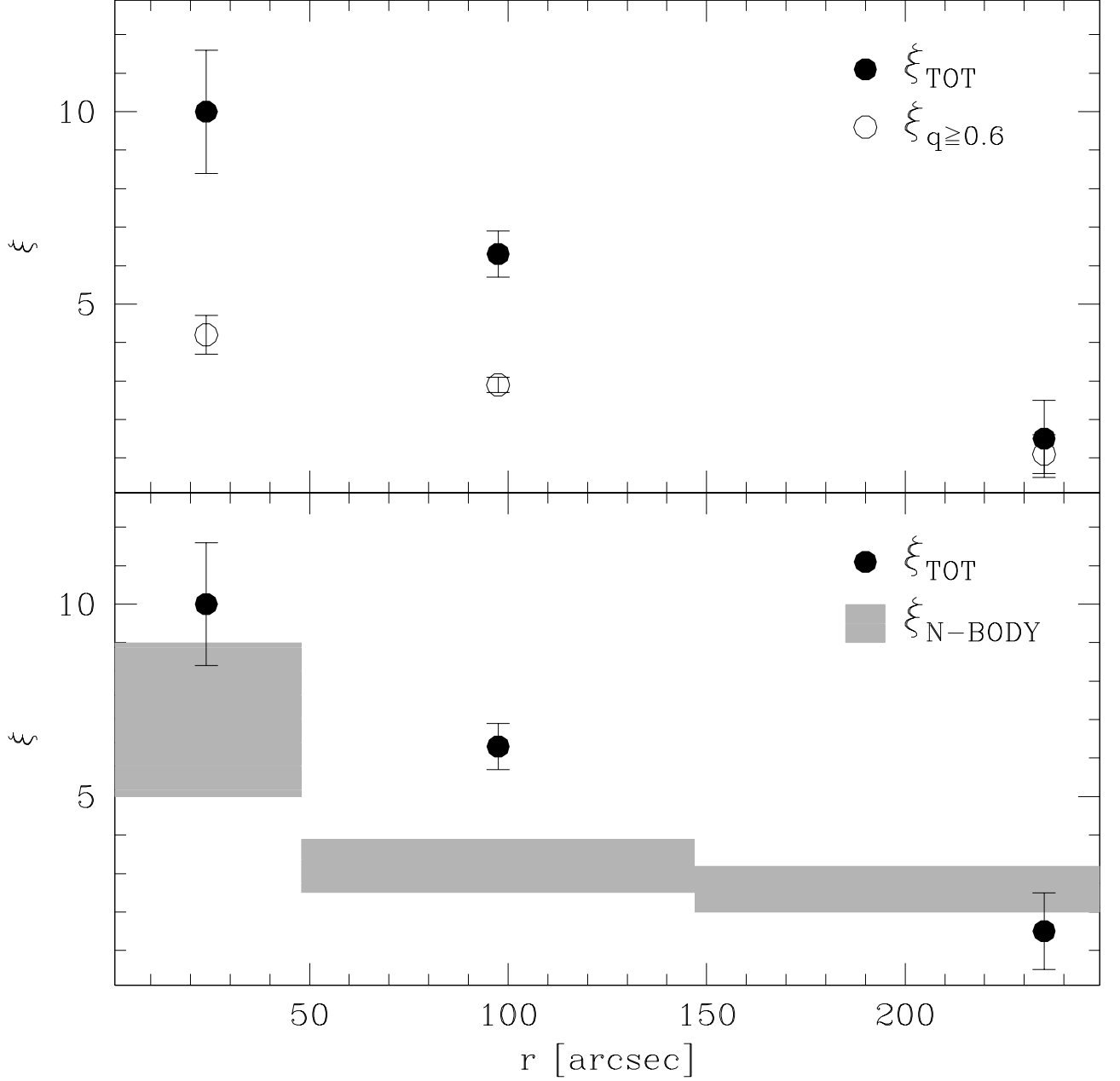


Fig. 7.— *Upper panel:* Radial behavior of the global binary fractions (black dots) and of the fraction of binaries with mass ratio  $q \geq 0.6$  (empty dots) estimated for the *intermediate* magnitude range ( $20.3 < I < 21.5$ ). *Lower panel:* comparison between the observed values of  $\xi_{\text{TOT}}$  (the same as above; black dots), and the corresponding current binary fractions obtained from an N-body simulation that started with a 5% primordial value and no central IMBH (gray regions; see text and B10).